A tritium catalytic fusion reactor concept

1998 Nucl. Fusion 38 1651

(http://iopscience.iop.org/0029-5515/38/11/305)

A TRITIUM CATALYTIC FUSION REACTOR CONCEPT

J.M. MARTÍNEZ-VAL[a], S. ELIEZER[a,b], Z. HENIS[b], M. PIERA[a,c]
[a] Institute of Nuclear Fusion,
Madrid Polytechnic University, Madrid,
Spain
[b] Soreq NRC, Yavne,
Israel
[c] ETSI Industriales, UNED, Madrid,
Spain

ABSTRACT. The performance of deuterium targets with small tritium seeding is analysed. The objective is to take advantage of the features of fusion reactivity ratios for very high burning temperatures in order to minimize tritium needs and to reduce the ignition temperature as much as possible. It is found theroretically and computationally that there is a regime for deuterium–tritium DT_x plasmas (with $x \approx 0.03$) where the final content of tritium in the pellet debris is the same as the initial contents in the original pellet. No external blankets to breed tritium would thus be needed. Although energy gains are limited because of the small fusion yield of DD reactions, the energy gain of DT_x targets is higher than that of pure deuterium plasmas. The ignition temperature and the driver energy are lower than the corresponding values of DD pellets. This concept is also very useful to reduce the tritium inventory and to simplify the complexity of inertial fusion reactors which use stoichiometric DT.

1. INTRODUCTION

Current proposals to burn the natural isotope deuterium (D) involve the use of tritium (T) in stoichiometric plasmas in order to have the minimum ignition temperature. Otherwise, for pure deuterium fuel, temperatures higher than 35 keV must be achieved in magnetic confinement plasmas, with Lawson parameters exceeding 10^{15} cm$^{-3} \cdot$ s. Similarly, in inertial confinement targets, the ignition temperatures must be over 20 keV in very thick (>2 g/cm^2) compressed plasmas, which require very large driver energies.

Tritium inventories in futuristic fusion reactors based on current stoichiometric DT proposals are very high, which poses a very significant radiological problem [1–4]. Besides that, tritium must be bred in external blankets of non-negligible complexity. In most of the designs, beryllium must be added as a neutron multiplier, which is an additional source of technological problems [5].

In this article, a new fuel for inertial fusion targets is proposed: pure deuterium with small tritium seeding. The general performance of tritium seeding in advanced fusion fuels has recently been reviewed in a systematic approach [6]. The aim of this article is to analyse in depth the performance of DT_x targets in order to find a catalytic regime for tritium burning, in such a way that no external tritium breeding is needed.

The burnup properties of DT_x fuel at high burning temperatures are analysed in Section 2, both theoretically and by computational means. The main finding in that section is the existence of a regime, corresponding to a range of x values around 0.025, where the final contents of tritium (in the pellet debris) are the same as the tritium contents in the original pellet.

The ignition conditions for DT_x targets are identified and computed in Section 3. Either spark ignition [7–10] or fast ignition [11] can produce very high energy gains with reasonable driver energy requirements. Volume ignition [12, 13] seems not suitable for this type of target, because the energy gains are rather small.

By using a standard model of propagated ignition [14–19], comparison among DT, DD and DT_x can be stated in a simple and clear way. Advantages from the use of DT_x fuel will then be evident. Albeit, ignition temperatures cannot be as low as the DT value, but they are much lower than in the pure DD case.

Some numerical examples of DT_x breedingless reactors will be given in Section 4. It will be shown that standard compressions of inertial fusion scenarios [20–30] are enough to achieve positive results in the performance of these targets. Compressions above

1000 times solid density already show a more than acceptable performance.

A summary of the work and some conclusions to guide further research on this topic are presented in Section 5.

2. BURNUP REGIMES OF DT_x PLASMA

At the stagnation phase (ignition onset) high temperature DT_x plasma isotopic evolution is mainly governed by the following equations:

$$\frac{dn_D}{dt} = -n_D^2\langle\sigma v\rangle_{DD} - n_D n_{He}\langle\sigma v\rangle_{DHe} - n_D n_T\langle\sigma v\rangle_{DT} \quad (1)$$

$$\frac{dn_{He}}{dt} = \frac{1}{4}\, n_D^2\langle\sigma v\rangle_{DD} - n_D n_{He}\langle\sigma v\rangle_{DHe} \quad (2)$$

$$\frac{dn_T}{dt} = \frac{1}{4}\, n_D^2\langle\sigma v\rangle_{DD} - n_D n_T\langle\sigma v\rangle_{DT} \quad (3)$$

where the subscripts stand for deuterium (D), tritium (T) and helium-3 (He). Additional reactions can be taken into account [6, 31] but they are of minor importance as compared with the former ones. Nevertheless, in the numerical computation to be presented, all possible fusion reactions are accounted for.

In the former equations it is worth mentioning that the $\langle\sigma v\rangle_{DD}$ reactivity is the standard one, defined as a double integral on the phase space of DD reacting particles [32, 33]. We consider both branches (yielding tritium and He-3) to have the same probability (50%). In turn, the first term of the RHS of Eq. (1) takes into account the fact that $\langle\sigma v\rangle_{DD}$ counts reacting particles, not reactions. In fact, the reaction rate is $\frac{1}{2}\, n_D^2\langle\sigma v\rangle_{DD}$, but we must take into account the fact that two deuterium nuclei are lost in this reaction.

As for the tritium concentration n_T, three different regimes can be distinguished:

(a) The breeder regime, $dn_T/dt > 0$,
(b) The burner regime, $dn_T/dt < 0$,
(c) The neutral or asymptotic regime, $dn_T/dt = 0$.

The last case will represent a minimum value of n_T if the previous phase was a burner regime. This is what happens at the beginning of the burning process, because the initial tritium nuclei are burnt up at a much higher speed than the deuterium nuclei.

On the contrary, $dn_T/dt = 0$ will represent a maximum if it occurs at the end of a breeder phase. It will also represent a dynamic equilibrium level once the tritium and deuterium concentrations become adjusted to the corresponding reactivities (which depend on the burning temperature, as will be seen below).

If N_T and N_D represent the total number of tritium and deuterium particles, we can write

$$\frac{N_T(t)}{N_T(0)} = \frac{N_T(t)}{N_D(0)}\,\frac{N_D(t)}{N_D(0)}\,\frac{N_D(0)}{N_T(0)}. \quad (4)$$

A catalytic regime of the target performance will require

$$N_T(\infty) = N_T(0) \quad (5)$$

where $N_T(\infty)$ is the tritium content in the pellet debris, i.e. for $t \to \infty$ (although the burnup lasts for much less than 1 ns).

On the RHS of Eq. (4), we have

$$\frac{N_D(0)}{N_T(0)} = \frac{1}{x} \quad (6)$$

$$N_D(\infty) = (1-\varphi)N_D(0) \quad (7)$$

where φ is the burnup fraction.

Therefore, we can define an index i of internal breeding

$$i = \frac{N_T(\infty)}{N_T(0)} = \frac{N_T(\infty)}{N_D(\infty)}\,\frac{(1-\varphi)}{x}. \quad (8)$$

From Eqs (1) and (3), in the asymptotic regime of the disassembly phase, the following relations hold:

$$\frac{N_T(\infty)}{N_D(\infty)} = \frac{n_T(\infty)}{n_D(\infty)} = \frac{\langle\sigma v\rangle_{DD}}{4\langle\sigma v\rangle_{DT}} = f_T. \quad (9)$$

This ratio depends quite a lot on the burning temperature, which in turn depends on the density of the compressed fuel at the ignition onset. Table I lists $\langle\sigma v\rangle_{DD}$, $\langle\sigma v\rangle_{DT}$ and f_T for some temperatures of interest.

Table I. Reactivity Values and f_T (Eq. (9)) Values at some Ion Temperatures

T (keV)	$\langle\sigma v\rangle_{DD}$ (cm^3/s)	$\langle\sigma v\rangle_{DT}$ (cm^3/s)	f_T
10	1.2×10^{-18}	1.1×10^{-16}	0.0027
100	4.5×10^{-17}	8.5×10^{-16}	0.013
200	8.8×10^{-17}	6.3×10^{-16}	0.035
250	1.1×10^{-16}	5.5×10^{-16}	0.05
300	1.2×10^{-16}	5.1×10^{-16}	0.06
400	1.5×10^{-16}	4.2×10^{-16}	0.09
500	1.8×10^{-16}	3.7×10^{-16}	0.12

It is worth remembering that the ion temperatures in a target microexplosion are much higher than the electron and radiation temperatures. The maximum ion temperatures in a DD target can reach 400 keV and above, but they go down as the target explodes and the thermal energy is transformed into kinetic energy. As a matter of fact, the burst will last some tens of picoseconds. Once the target starts exploding, the density goes down so rapidly that no additional fusion reactions take place, as will be seen later, with some numerical results.

From Eqs (4)–(9), the following relations hold:

$$i = \frac{N_{\mathrm{T}}(\infty)}{N_{\mathrm{T}}(0)} = f_{\mathrm{T}}\,\frac{1-\varphi}{x}. \tag{10}$$

Therefore, in order to have self-breeding, the initial tritium content x must be

$$x = f_{\mathrm{T}}(1-\varphi). \tag{11}$$

From Table I and Eqs (8) and (9), it can be seen that a burnup fraction of 40% ($1-\varphi = 0.6$) and a burning temperature of 250 keV will produce a catalytic regime for $x = 0.03$ ($N_{\mathrm{T}}(\infty) = N_{\mathrm{T}}(0)$). This theoretical estimate fits quite well with the numerical results given below, that take into account all the fusion reactions in the plasma and its mechanical disassembly. The computational code used to carry out these calculations has been previously reported [6] and includes a simulation of the expansion process that agrees quite well with more sophisticated fluid equation calculations [21, 24, 34, 35].

Figure 1 shows the evolution of the number of particles of different species in an exploding target with the following specifications at the ignition onset:

(a) DT_x, with $x = 0.025$.
(b) Density: 500 g/cm^3.
(c) Temperature: 10 keV.
(d) ρR: 15 g/cm^2.

It is worth pointing out that the final tritium content (in number of particles) is practically the same as the initial one. A better representation of the tritium evolution is given in Fig. 2, where a tritium burning phase is seen at first, due to which ignition starts at a low temperature (in fact the initial ignition temperature in the spark can be as low as 8 keV for $x = 0.025$). Afterwards, the number of tritium particles increases to a higher value than the original one and immediately tends to the equilibrium value corresponding to the burning temperature. The time evolutions of the ion and electron average temperatures are depicted in Fig. 3.

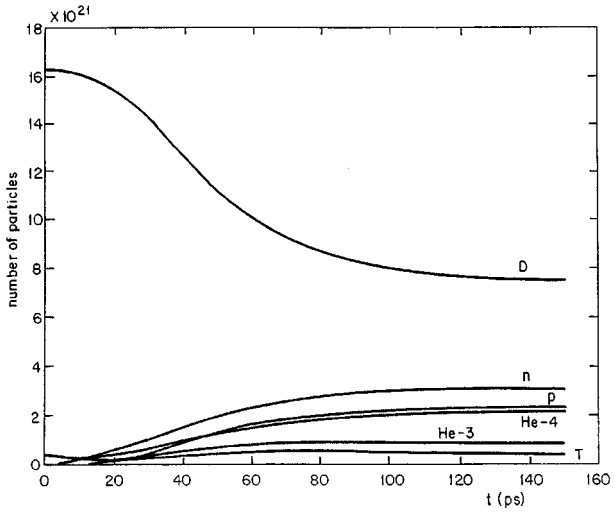

FIG. 1. Time evolutions of the numbers of particles of different ion species in the burnup of a DT_x spherical target with the following specifications at the ignition onset: $x = 0.025$, $\rho = 500$ g/cm^3, $\rho R = 15$ g/cm^2, $T_{\mathrm{i}} = 10$ keV.

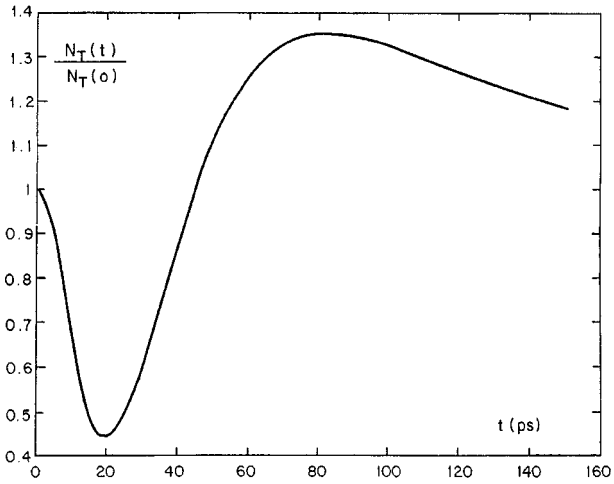

FIG. 2. Relative tritium content in the pellet of Fig. 1 along burnup.

Equations governing these temperatures have already been reported [6], but it is important to justify by simple estimates that the ignition temperature for the DT_x case is much lower than that for the DD case. As a first approach let us ignore the contribution of DD until the temperature reaches 35 keV. This means that DT reactions have to heat the plasma from the ignition temperature up to 35 keV. As a matter of fact, the heating must be supersonic in order to trigger the fusion burst before the mechanical expansion of the target begins (i.e. the heating time must be shorter than the confinement time). An accurate calculation of the ignition temperature will

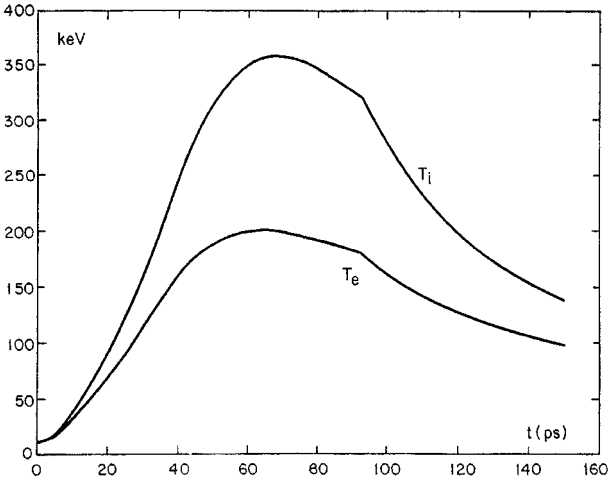

FIG. 3. Time evolutions of the ion and electron temperatures in the case described in Fig. 1.

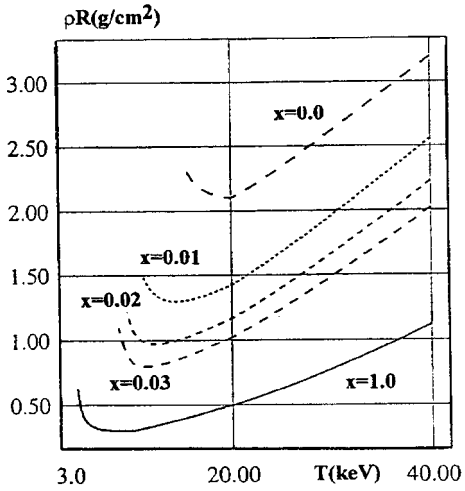

FIG. 4. Minimum ignition conditions for propagated ignition in DT_x plasmas, for different x values. T corresponds to T_s (Eq. (39)). The left hand ends of the lines indicate the minimum ignition temperature (below which, radiation losses make ignition impossible if radiation reabsorption is not taken into account). (The scales on both axes are linear.)

be presented in the next section. For the moment, we will require the plasma reheating by 3.5 MeV alpha particles to be larger than the bremsstrahlung losses. In short, this condition can be expressed as

$$r_{DT} n_D n_T > b(n_D + n_T)^2 \tag{12}$$

where r_{DT} is a function of the temperature (through the reactivity) and b is a radiation function behaving as $T^{1/2}$. It can be rewritten as

$$x r_{DT} > b(1+x)^2. \tag{13}$$

Hence

$$\frac{r_{DT}}{b} > \frac{(1+x^2)}{x} \tag{14}$$

and we also know that the ignition temperature for $x = 1$ is $T = 4.5$ keV. In the range close to 10 keV, r_{DT} behaves as T^4, while b always behaves as $T^{1/2}$. Thus, the former ratio can be expressed in terms of the temperature,

$$\left(\frac{T_x}{4.5}\right)^{3.5} > \frac{(1+x)^2}{4x} \tag{15}$$

where T_x (keV) is the ignition temperature for DT_x. For $x = 0.03$, the ignition temperature defined in this simplistic way is 8.5 keV. This value is in good agreement with the more accurate calculations summarized in Fig. 4.

In order to heat the plasma from 8.5 up to 35 keV for the DD reactions to be self-powered, the number of particles to heat is $2n_D(1+x)$ cm^{-3}, which means about $75n_D(1+x)$ keV/cm^3 of heating energy. If we only account for one 3.5 MeV alpha particle per reacting tritium, the requirement is

$$3500\varphi_T x > 75(1+x) \tag{16}$$

where φ_T is the tritium burnup in the initial burning phase. Therefore

$$1 > \varphi_T \geq \frac{1+x}{47x}. \tag{17}$$

For instance, for $x = 0.03$, $\varphi_T \geq 0.73$. On the other hand, $\varphi_T < 1$ implies $x > 0.02$, which represents a lower boundary for triggering ignition just by burning the initial tritium contents. These estimates are very rough, and more accurate figures will be given in the numerical calculations of the following sections. Nevertheless, the former estimates are easy to follow and they justify why the ignition temperature in DT_x is much smaller than that in pure DD, even for very small x values.

3. IGNITION REQUIREMENTS FOR DT_x PELLETS

Several ignition schemes have been identified in inertial fusion, namely

(a) Volume ignition [12, 13], where most of the compressed pellet starts fusion burning at the same time. It corresponds to compressed targets with very

uniform temperatures and density profiles inside the target.

(b) Spark ignition [7–10], where the central core of the compressed target reaches very high temperatures (higher than 5 keV for DT capsules) at moderate densities, while the bulk of the fuel (∼90% of it) remains at much lower temperature but at much higher density (with an almost uniform pressure profile).

(c) Stimulated ignition [11, 36] where an external source of energy is used to create a spark in an already compressed target, from which ignition propagates. The so-called fast ignition [11] is based on heating the spark by an ultrashort laser beam of very high power. Another possibility is the use of microscopic plasma jets to trigger ignition by hypervelocity impact [37]. A third option is the use of a charged particle accelerated beam.

The last two cases (b) and (c) correspond to propagated ignition. Cold plasma surrounding the spark must be heated to burning temperatures by electron heat conduction and fusion born particle energy deposition before its mechanical disassembly. The propagation of the fusion burning wave must be highly supersonic. Moreover, spark temperature and size must be high enough to overheat the spark and at the same time to launch the supersonic fusion burning wave. These criteria will be analysed afterwards, once the energy mechanisms involved in ignition and burn propagation are discussed.

3.1. Energy mechanisms

In inertial fusion target performance we must take into account

- Hydrodynamic motion,
- Radiation,
- Electron heat conduction,
- Fusion born particle energy deposition.

Other effects such as suprathermal fusion are negligible in this context [38].

3.1.1. Hydrodynamic forces

There are two energy terms related to the hydrodynamic motion which must be considered in the target evolution:

- Compression work, $p\,\mathrm{d}V$,
- Kinetic energy density, $\rho v^2/2$,

where p is the pressure, V the specific volume, ρ the density and v the speed. These terms are fundamental ones during the implosion phase, where the fuel and the pusher reach very high speeds (in general, over 3×10^7 cm/s). The compression work is mainly important in the stagnation phase, in creating a spark due to the piston-like action of the pusher and outer fuel over the innermost fuel core.

In the model for propagated ignition that we are going to discuss in this section, a uniform pressure profile is assumed along the stagnation phase, i.e. the moment of maximum internal energy density in the fuel [26]. Hence, hydrodynamic forces will not play any direct role in assessing the ignition criterion. In other words, the implosion history will not be included in the analytical model. Implosion simulations by numerical computation have been reported several times [18, 21, 24], and the type of implosion history needed to arrive at a given compressed state is known.

Nevertheless, hydrodynamic forces must be taken into account in the fusion propagation model, because propagation must be supersonic. In hot deuterium plasmas, the speed of sound is

$$3.8 \times 10^7\ \mathrm{T}^{1/2} \cdot \mathrm{cm/s} \tag{18}$$

with T in kiloelectronvolts. For DT stoichiometric plasmas, it is

$$3.4 \times 10^7\ \mathrm{T}^{1/2} \cdot \mathrm{cm/s}. \tag{19}$$

Therefore, if the bulk of the fuel is a DT_x plasma ($x \ll 1$) at 1 keV, a fusion burning wave must run faster than 4×10^7 cm/s. In fact, the wave speed will be dominated by the slowing down features of fusion born charged particles and knock-on ions, and it will be higher than 4×10^8 cm/s [7, 36].

3.1.2. Radiation

This is a major loss term in any hot plasma. For a hydrogen plasma, it is

$$B\left(\frac{W}{\mathrm{cm}^3}\right) = 5.35 \times 10^{-31} n_\mathrm{e} n_\mathrm{i} T^{1/2} \tag{20}$$

with T in kiloelectronvolts. If the relation between n_e, n_i and density ρ (g/cm^3) is taken into account for a DT_x plasma (for any x value) we can write

$$B\left(\frac{W}{\mathrm{cm}^3}\right) = 1.92 \times 10^{17}\,\frac{(1+x)^2}{(2+3x)^2}\,\rho^2 T^{1/2}. \tag{21}$$

The temperature profile inside the spark will not be uniform, but that effect will properly be taken into account when establishing the ignition criterion in Section 3.2.

3.1.3. Electron heat conduction

The temperature profile of a thermally expanding spark will follow the profile [18, 19]

$$T(r) = T_0 \left[1 - \left(\frac{r}{r_0} \right)^2 \right]^{2/7} \tag{22}$$

where T_0 is the central (maximum) temperature and r_0 is the spark radius.

This profile can be used to compute the thermal conduction from the spark, according to the Spitzer formulation

$$Q\left(\frac{W}{\mathrm{cm}^2}\right) = -k\nabla T = -\frac{9.4 \times 10^{12}}{Z \ln \Lambda} T^{5/2} \nabla T. \tag{23}$$

From Eq. (22), the gradient can be substituted by

$$\nabla T = -\frac{4}{7} \frac{T_0}{r_0}. \tag{24}$$

If Eq. (23) for the thermal flux is integrated over $4\pi r_0^2$, one obtains

$$H\ (\mathrm{W}) = 4\pi r_0^2 Q = \frac{6.75 \times 10^{13}}{\ln \Lambda} T_0^{7/2} r_0 \tag{25}$$

where the Coulomb logarithm is taken from Ref. [39].

It is worth underlining that integration of bremsstrahlung losses, Eq. (21), in the volume of the spark leads to an expression depending on $\rho^2 r_0^3$, while H depends only on r_0. The factor $(\rho r_0)^2$ will play a very important role in the ignition criterion.

3.1.4. Fusion-born particle energy deposition

Charged particles will deposit their energy according to the stopping power of the background plasma, which mainly depends on density and temperature. If the particle range is expressed in terms of areal density (ρR), it is almost independent of the density. For very hot plasmas ($T_\mathrm{e} \gg 30$ keV) the stopping power is dominated by ion collisions, and it is almost independent of the ion temperature. For $T_\mathrm{e} < 30$ keV, which is the case for DT_x ignition, the stopping power is dominated by electrons [15, 40] and the range of the 3.5 MeV alpha particles can be expressed as

$$\rho R_\alpha\ (\mathrm{g/cm}^2) = 0.04 T^{3/2} \tag{26}$$

with T in kiloelectronvolts. Similar formulas can be found for other particles and knock-on ions [15]. This means that a fraction of the alpha particle energy will be deposited out of the spark. That deposition will heat the surrounding fuel and will pump the fusion burning wave. Alpha particle transport and slowing down can be studied with Fokker–Planck codes and similar tools [41], but simple estimates are also given in the literature to evaluate the escape fraction [15].

In DT_x fuels, the fusion power will have two components: DT reactions and DD reactions with subsequent burnup of the tritium and He-3 particles. The reheating power inside the spark will be described as

$$F\ (\mathrm{W}) = F_\mathrm{T}\ (\mathrm{W}) + F_\mathrm{D}\ (\mathrm{W}) \tag{27}$$

where

$$F_\mathrm{T} = E_\mathrm{T} \int_0^{r_0} 4\pi r^2 n_\mathrm{D} n_\mathrm{T} \langle \sigma v \rangle_\mathrm{DT}\, \mathrm{d}r \tag{28}$$

$$F_\mathrm{D} = E_\mathrm{D} \int_0^{r} 4\pi r^2 n_\mathrm{D}^2 \langle \sigma v \rangle_\mathrm{DD}\, \mathrm{d}r \tag{29}$$

where E_T and E_D are the energies deposited inside the spark by fusion born particles, including neutrons through elastic collisions with the background ions (deuterium mainly) [41]. The former integration has to take into account the temperature profile given in Eq. (22), as will be seen in Section 3.2.

In order to compute E_T and E_D, the charged particle contribution can be determined by comparison of the particle range R_p and the spark radius r_0. At ignition onset, the fraction of energy deposited into the spark can be taken as

$$\xi = 1 - \left(1 - \frac{r_0}{R_\mathrm{p}} \right)^2 \tag{30}$$

for $R_\mathrm{p} \geq r_0$, with the obvious limitation $\xi = 1$ for $R_\mathrm{p} \leq r_0$. Exact solutions for ξ in homogeneous plasmas can be found in Ref. [15].

Fourteen MeV neutrons flowing in a deuterium plasma of ρr_0 areal density will deposit an energy estimated by Ref. [41] to be

$$\frac{14 \rho r_0}{13.72 + \rho r_0}\ (\mathrm{MeV}) \tag{31}$$

and 2.45 MeV neutrons (from 50% of DD reactions) will deposit the following amount of energy through knock-on ions:

$$\frac{2.45 \rho r_0}{3.92 + \rho r_0}\ (\mathrm{MeV}). \tag{32}$$

The neutron contribution to reheating is negligible for ρr_0 much smaller than 1 g/cm^2, but it becomes sizeable for areal densities about 1 g/cm^2 and higher, and must be taken into account.

As in the integration of radiation emission in the spark volume, the integrals of Eqs (28) and (29) also depend on $\rho^2 r_0^3$, because n_D has the following form:

$$n_D = \rho \frac{0.6 \times 10^{24}}{2 + 3x}. \quad (33)$$

Therefore, both total bremsstrahlung losses and fusion reheat do depend on $\rho^2 r_0^3$, while heat conduction only depends on r_0. This will be very important for the ignition criterion.

3.2. Ignition criterion

Let us assume that a spark has been created inside a compressed target, either by the inherent features of the implosion history or by the action of an additional igniting beam. The spark will be characterized by T_0 and r_0 (Eq. (22)), and by the density ρ_0, that can be equal to the density of the bulk of the fuel (isochoric mode) or somewhat lower (isobaric mode).

The total internal energy in the spark will be

$$E_i = \int_0^{r_0} \frac{3}{2} (n_e + n_i) T(r) 4\pi r^2 \, dr \quad (34)$$

$$E_i = 6\pi (n_e + n_i) T_0 \int_0^{r_0} \left(\frac{r_0^2 - r^2}{r_0^2} \right)^{2/7} r^2 \, dr \quad (35)$$

which can be rearranged as

$$E_i = 3\pi r_0^3 (n_e + n_i) T_0 I_E \quad (36)$$

where

$$I_E = \int_0^1 y^{2/7} (1 - y)^{1/2} \, dy = 0.4814. \quad (37)$$

If the internal energy is expressed in terms of an effective spark temperature T_s,

$$E_i = \frac{4}{3} \pi r_0^3 (n_e + n_i) \frac{3}{2} T_s \quad (38)$$

and it is easy to identify

$$T_s = \frac{3}{2} T_0 I_E = 0.72 T_0. \quad (39)$$

Similarly, radiation losses can be computed by integration of Eq. (21), and an effective radiation temperature is defined as

$$T_r^{1/2} = \frac{3}{2} T_0^{1/2} I_B \quad (40)$$

where

$$I_B = \int_0^1 y^{1/7} (1 - y)^{1/2} \, dy = 0.5613. \quad (41)$$

Hence

$$T_r = 0.71 T_0 \quad (42)$$

which is very similar to T_s.

The total radiation loss L (W) is

$$L \text{ (W)} = \int_0^{r_0} B(r) 4\pi r^2 \, dr \quad (43)$$

which yields

$$L \text{ (W)} = 6.15 \times 10^{16} r_0^3 \rho^2 T_0^{1/2} I_B \frac{25}{4} \frac{(1 + x)^2}{(2 + 3x)^2} \quad (44)$$

where r_0 and ρ are in CGS units and T_0 in kiloelectronvolts.

It should be remembered that the radiation loss cannot exceed the emission of a black body. Therefore, when the volume of the plasma becomes large enough, it behaves as a black body, and a significant part of the original bremsstrahlung radiation is reabsorbed, in such a way that the actual loss is

$$L \text{ (W)} = 4\pi r_0^2 \sigma T_e^4 \quad (45)$$

where T_e is the surface temperature and σ is the Stefan–Boltzmann constant. Because of the former limitation, it can be stated that a deuterium plasma sphere will become a black body if its density, radius and temperature meet the following criterion:

$$\rho^2 r_0 > 7.25 \times T_r^{7/2} \quad (46)$$

(for ρ and r_0 in CGS units and T_r in kiloelectronvolts).

If we considered plasma densities of about 400 g/cm^3 and $T_r \approx 10$ keV, the areal density of the plasma to become a black body would be $\approx$55 g/cm^2. We will see that the areal densities required to ignite DT_x targets will be much lower than 55 g/cm^2. Therefore, radiation reabsorption will be negligible inside the spark.

Equation (25) for electron heat conduction from the spark, Eq. (27) for fusion reheating and Eq. (43) for bremsstrahlung emission will be taken into account to establish the ignition criterion as follows:

Fusion reheating by fusion born particle energy deposition inside the spark must be larger than bremsstrahlung plus heat conduction losses,

$$F > L + H. \quad (47)$$

In addition to that, two additional criteria must be met:

(a) The heating time from the ignition temperature up to 40 keV (full DD burst) must be shorter than the stagnation time of the spark ($\sim r_0/c_s$).

(b) The fusion-burning wave propagation speed must exceed the speed of sound of the compressed plasma.

In fact, both additional criteria are easily met if the first is fulfilled in a DT_x plasma. The heating time can be expressed as [12]

$$t_h = \int_{T_s}^{40} \frac{3}{2}(n_e + n_i)\,\frac{4}{3}\,\pi r_0^3 (F - L - H)^{-1}\,dT. \quad (48)$$

A suitable parameter to characterize the plasma reheating can be defined by

$$\gamma = \frac{F - L - H}{F} \quad (49)$$

which has a positive value when ignition criterion (47) is fulfilled.

If Eq. (27) is taken into account for the definition of F, and $\langle\sigma v\rangle_{DT}$ is expressed as a function proportional to a power of temperature $\langle\sigma v\rangle_{DT} \sim T^{m+1}$, the confinement time is found to scale as

$$t_h \approx \gamma^{-1}\rho^{-1}T^{-m} \quad (50)$$

where the exponent m is much higher than 0.5, because of the dependence of the reactivity $\langle\sigma v\rangle_{DT}$ on the temperature. On the other hand,

$$t_s \approx \frac{r_0}{4c_s} = \frac{\rho r_0}{4\rho c_s} = c(\rho r_0)\rho^{-1}T^{-1/2} \quad (51)$$

and hence

$$\frac{t_h}{t_s} \approx \gamma^{-1}T^{-m+1/2}(\rho r_0)^{-1}. \quad (52)$$

It can be seen that once T and ρr_0 fulfil the ignition criterion stated by Eq. (47), γ increases very rapidly as T and/or ρr_0 increase, so giving a ratio t_h/t_s as small as needed. On the other hand, the propagation speed of the fusion burning wave will depend on the time needed to heat the surrounding cold fuel by alpha particle transport and by electron heat conduction.

The heating speed from the electron heat conduction can be computed from the following expression:

$$Q\left(\frac{W}{cm^2}\right) = C_p\left(\frac{J}{g\cdot keV}\right)\rho\left(\frac{g}{cm^3}\right)v\left(\frac{cm}{s}\right)T_s\ (keV) \quad (53)$$

where $T_s \approx 10$ keV for the DT_x plasma under study, and Q was defined in Eq. (21), which can be expressed as $qT_0^{7/2}r_0^{-1}$. For an ideal gas equation of state

$$C_p = \frac{2.88\times 10^8(1+x)}{2+3x}\ (J/g\cdot keV). \quad (54)$$

Therefore, the heating speed of the electron conduction wave is (for $\ln\Lambda \approx 2$ and $x \approx 0.03$)

$$v_h \approx 2.8\times 10^4 T_0^{5/2}(\rho r_0)^{-1} \quad (55)$$

which is an important mechanism for small sparks (small areal densities). For instance, for $T_0 = 12$ keV and $\rho r_0 = 0.33$ g/cm^2, which are suitable values for stoichiometric DT [18, 19], the heating speed is about 4.5×10^7 cm/s (see Eq. (19)).

Charged particle transport and energy deposition become a much more important mechanism for ignition propagation when the spark is large. In a linear approach (that does not take into account the Bragg peak, but is a good estimate for analytical purposes) the propagation speed v_α scales as

$$v_\alpha \approx \rho\,\frac{\langle\sigma v\rangle_{DT}}{T_b} \quad (56)$$

where T_b is the temperature needed for ignition propagation, which is about 10 keV for DT_x plasmas ($x \approx 0.03$). It will be assessed after computing ignition conditions for DT_x that v_α will be high enough to propagate ignition across the cold plasma. As a matter of fact, the speed given in Eq. (56) is inherently limited by the slowing down of the alpha particles, which have an effective speed somewhat higher than 4×10^8 cm/s [40].

3.2.1. Computation of minimum ignition conditions

The criterion

$$F \geq L + H \quad (57)$$

can easily be computed for any x of DT_x plasmas. In fact, for a T_s given by Eq. (39) it is possible to obtain the ρr_0 that satisfies the equality of Eq. (57). For points in the $(T, \rho r_0)$ plane over this line, ignition is possible. Of course, there is a minimum T_s below which ignition is impossible because of radiation losses. The line of minimum ignition conditions is shown in Fig. 4.

It is also easy to see that heat conduction losses dominate over bremsstrahlung emission for small ρr_0. For instance, for $x = 0.03$, the line in the log–log plane of $(T_0, \rho r_0)$,

$$\log(\rho r_0) = \frac{3}{2}\log(T_0) - 2 \quad (58)$$

indicates the border between the regions where each loss mechanism is dominant (T_0 in kiloelectronvolts, ρr_0 in g/cm^2). For large ρr_0 and small T_0 (from that line) radiation dominates. For high T_0 and small ρr_0,

heat conduction dominates. For instance, for $\rho r_0 = 1$ g/cm^2, the corresponding temperature of that line is $\log(T_0) = 4/3$ ($T_0 = 21.5$ keV).

The application of the ignition criterion of Eq. (47) to a DT$_x$ plasma of a given x is shown in Fig. 4 in the $(T, \rho R)$ plane. For each curve (each x value) ignition is possible above that line and not possible below it. The parabolic shape of the curves stems from the dependence of F, L and H on the plasma parameters $(T, \rho R)$ as established in Eqs (25), (27) and (44). It is also found that, for every x, there is a minimum value of ignition T, for which $\rho R \to \infty$.

From Fig. 4, it is evident that small tritium seeding of deuterium plasmas is actually very positive in relaxing the ignition conditions. Ignition temperatures are reduced from 20 keV for $x = 0.0$ to 7 keV for $x = 0.03$, and the areal density is reduced from more than 2 g/cm^2 to less than 1. The region of the tritium catalytic regime $x \approx 0.025$ presents much better conditions for ignition than pure DD.

Figure 5 is very relevant in this context, because it presents the spark internal energy. Savings in internal energy are impressive when adding some tritium. As a reference, stoichiometric DT ignition requires one thousand times less energy than stoichiometric DD ignition. This is of paramount importance.

It is also very important to observe the fact that tritium seeding with $x = 0.03$ reduces the energy requirements for ignition by a factor of 33 from the DD value. Of course, this means a much lower driver beam energy, which is a fundamental issue in inertial fusion.

The spark maximum gain is depicted in Fig. 6, for lines given in Fig. 4. Gain is defined as the maximum yield from the spark (if all tritium nuclei undergo fusion with deuterium nuclei, and the remaining deuterium nuclei undergo fusion with themselves and with the fusion born tritium and He-3 ions, in such a way that 6 MeV per deuterium ion appears from the plasma).

It is very important to observe that the catalytic regime also presents the advantage of increasing the energy gain. In fact, the DD gain is rather limited, because of its very high ignition requirements and moderate fusion yield. Figure 7 presents the maximum spark gain for different ignition conditions in several DT$_x$ fuel mixtures. For every ignition temperature (abscissa) an areal density is needed, according to the values given in Fig. 4. It is worth noting that the above mentioned spark gain is not the

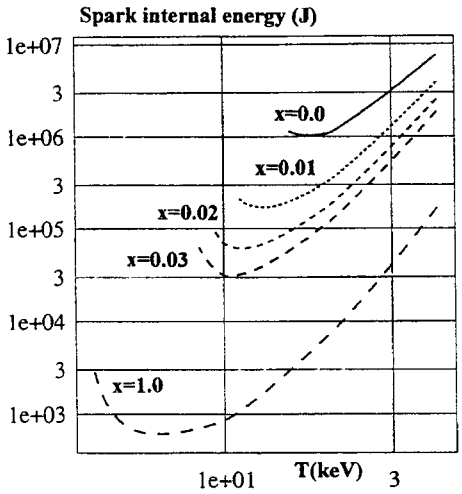

FIG. 5. Spark internal energy J for lines of the minimum ignition condition given in Fig. 4 (log–log scale).

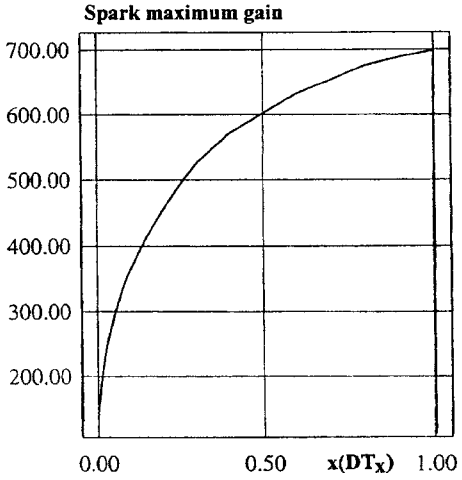

FIG. 6. Spark maximum gain for best ignition conditions given in Fig. 4, computed as the maximum spark yield divided by the spark internal energy.

total energy gain of the target, because it only takes into account the fusion energy produced in the initially ignited target. In general, both for internally produced sparks or for fast ignited ones, ignition will propagate from the ignitor (or spark) to the bulk of the fuel, and the fusion yield will be much higher than the mere yield from the spark, which will substantially be used to propagate ignition. In a general estimate, the total fusion yield will be 10 times as large as the spark yield, and therefore the target gain will also be ten times larger. For instance, for DT$_{0.02}$, the gain can reach 2000, a value high enough for a reactor scenario. However, for pure DD, the gain will be limited to 1000 or less.

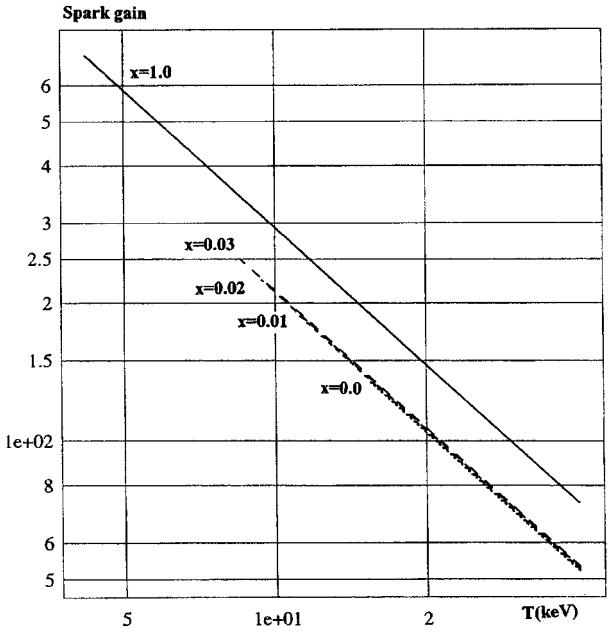

FIG. 7. Maximum spark gain for different target compositions (x), depending on the ignition temperature (in turn depending on the areal density of the compressed target, as indicated in Fig. 4).

3.3. DD capsules with a central DT core

An alternative to the earlier scheme of the DT_x target would be a double layer target with an inner layer of stoichiometric DT and an outer, larger, layer of DD. The burnup performance would have to be tuned in such a way that the final content of tritium in the pellet debris be the same as the initial one. Of course, reprocessing of the target debris would be rather complex, because some isotope separation between tritium and deuterium would be needed in order to make the DT stoichiometric material. Moreover, mixing between the layers could reduce the effectiveness of this idea.

This type of DD target with a central core of stoichiometric DT was analysed by Miley and others [42–44], but a homogeneous DT_x plasma was never considered (Fig. 6 of Ref. [42]). One of the critical issues of a two layered target is the material mixing between the layers in the deceleration phase at the end of the implosion, but this topic was not addressed in the cited bibliography.

In Ref. [42], page 314, catalysed deuterium refers to a plasma where the tritium and He-3 products from DD reactions thermalize in the plasma and react with deuterium at the same rate as they are produced. This general statement is not related to the ignition process and the ignition requirements, which are the fundamental points of our article.

Catalysed deuterium reactors were analysed in Ref. [45] without any reference to the igniton problem, because it is only related to the tritium and He-3 slowing down within the reacting plasma and subsequent burning in DT and DHe-3 reactions.

It is worth pointing out that our proposal for DT_x catalytic targets only works for plasmas with a very high burning temperature, above 200 keV (Eq. (10) and Table I). However, the catalytic deuterium process can take place also at low temperature within the fusion domain, i.e. 10 keV or so, and it is therefore compatible with the anticipated burning temperatures of magnetic confinement reactors.

4. NUMERICAL SIMULATION OF DT_x TARGET BURNUP

The performance of DT_x targets has been analysed by means of a simulation model [6] based on the nuclei depletion and ion and electron energy equations. The total content of the ith ion species is governed by

$$\frac{\mathrm{d}N_i}{\mathrm{d}t} = \sum_{j=1}^{m} a_i^j N_{j(1)} N_{j(2)} \langle \sigma v \rangle_j \, \frac{1}{V} \tag{59}$$

where V is the volume of the pellet at a given moment, N_i is the total number of particles of type i in the pellet, j is a reaction index (to take into account all the relevant reactions in the plasma [31]) and a_i^j is the effect of reaction j on nucleus i (it is 1 when particle i is produced in reaction j; -1 when it is a reactant, and 0 otherwise). $\langle \sigma v \rangle_j$ is the Maxwellian reactivity of reaction j, which depends on the ion temperature given by

$$\begin{aligned} &\frac{3}{2} \frac{\mathrm{d}}{\mathrm{d}t} \left(\sum_i N_i T_i \right) \\ &\quad = \sum_{j=1}^{m} \sum_k f_k^i w_k^j E_j N_{j(1)} N_{j(2)} \langle \sigma v \rangle_j \, \frac{1}{V} \\ &\qquad - \frac{P_{\mathrm{ie}}}{V} - \frac{\sum_j N_j T_j}{V} \, 4\pi R^2(t) c_{\mathrm{s}} \end{aligned} \tag{60}$$

where T_i is the ion temperature, f_k^j is the fraction of the energy of reaction product k deposited in the plasma ions, E_j is the total energy output of reaction j, w_k^j is the fraction of E_j carried by product k (for instance, 0.2 for the alpha particle created in the DT

reaction, where $E_j = 17.6$ MeV). P_{ie} stands for the ion–electron exchange term, given by

$$P_{ie}\ (\mathrm{keV \cdot cm^3/s}) = 1.69 \times 10^{-13} N_e \sum_i \ln \Lambda_i Z_i^2 \frac{N_i}{m_i} \frac{T_i - T_e}{T_e^{3/2}} \qquad (61)$$

where N_e is the total number of electrons, Z_i is the atomic number of ion species i, with a mass m_i, and $\ln \Lambda_i$ is the corresponding Coulombian logarithm [6, 38]. The ion and electron temperatures T_i and T_e are given in kiloelectronvolts. The electron energy equation is

$$\frac{3}{2}\frac{\mathrm{d}}{\mathrm{d}t}(N_e T_e) = \sum_{j=1}^{m}\sum_k (1 - f_k^j) w_k^j E_j N_{j(1)} N_{j(2)} \langle \sigma v \rangle_j \frac{1}{V} + \frac{P_{ie}}{V} - \frac{P_B}{V} - \frac{N_e T_e}{V} 4\pi R^2(t) c_s \qquad (62)$$

where c_s is the speed of sound in the plasma and P_B/V is the bremsstrahlung emission (integrated in the full target)

$$P_B\ (\mathrm{keV \cdot cm^3/s}) = 2.94 \times 10^{-15} N_e \sum_i N_i Z_i^2 T_e^{0.5}. \qquad (63)$$

The radius is assumed to expand as

$$R(t) = R(t - \Delta t) + v_{exp} \Delta t \qquad (64)$$

once ignition starts, where the expansion speed v_{exp} is connected to c_s, which is computed by

$$c_s = \left(\frac{\gamma P}{\rho}\right)^{1/2} \qquad (65)$$

including both the ion and the electron pressure in P, with $\gamma = 5/3$.

The expansion speed is

$$v_{exp} = \eta c_s \qquad (66)$$

where η is a factor depending on the burnup that increases linearly from 0 to 1 as the burnup fraction φ increases from 0 to 0.5, and η remains 1 for $\varphi > 0.5$. This phenomenological recipe agrees quite well with space dependent simulation of target explosions [15, 21, 24].

This type of lumped model enables us to make a very broad analysis of the burnup performance of DT_x targets. It is obvious that more accurate results for a definite target would require two dimensional computer codes to simulate implosion nonuniformities, hydrodynamic instabilities and related phenomena, but the formerly described model is a suitable one to determine the burnup features of DT_x targets and the main parameters affecting the tritium catalytic regime, because this model focuses on the equations governing the reaction rates.

It is important to use a two temperature model because T_e and T_i separate once they are above 30 keV. This is properly taken into account by the coefficients f_k^j and $1 - f_k^j$ in the T_i and T_e equations. These coefficients have been calculated with an exact formulation [46], but an average value for charged particle energy deposition is

$$1 - f = \frac{150}{150 + T_e^{1.5}} \qquad (67)$$

with T_e in kiloelectronvolts.

Both energy equations are connected through the ion–electron collision term P_{ie}. Another fundamental mechanism is the target explosion, which is characterized by Eqs (64) to (66), and it is represented by last terms of the energy, Eqs (60) and (62).

Because of the very high densities of the compressed targets, the fusion burst lasts about 100 ps or less. This is clearly seen in Figs 1 to 3, which correspond to a fuel density of 500 g/cm^3.

Increasing the density by producing stronger compressions in the implosion process does not help much to widen the design window for the catalytic regime, but it can be very important in order to reduce the fuel mass, and therefore to reduce the driver energy and the fusion yield, which must be limited by technological problems of the reactor chamber [1, 2]. It must be remembered that fuel mass decreases as ρ^{-2} for constant ρR, which is a dominant parameter in determining ignition temperature, as was shown in the analysis of Section 3.

At higher densities, the burning ignition temperatures are somewhat higher and the burst time is slightly shorter, if ρR is kept constant. The tritium ratio $N_T(\infty)/N_T(0)$ decreases a little with increasing density, but reaches a saturation level even for very high densities. For instance, in a set of cases with variable density and fixed $\rho R = 15$ g/cm^2, for $x = 0.025$ and initial bursting temperature $T_i = 25$ keV, results are given in Table II. The tritium index decreases from 1.05 to 0.97 when the density increases from 500 to 2000 g/cm^3. The burnup fraction and burning temperature increase by small factors.

Table II. Tritium Index i ($N_T(\infty)/N_T(0)$) and Maximum Ion Temperature for Different Target Densities with the Following Fixed Specifications: $\rho R = 15$ g/cm^2, $T_{i0} = 25$ keV. Initial Tritium Contents, $x = 0.025$

Density (g/cm^3)	Radius (μm)	Tritium index, i	Maximum ion temp. (keV)	Burnup fraction
500	300	1.04	376	0.54
2000	75	0.97	380	0.55
7500	20	0.97	383	0.55

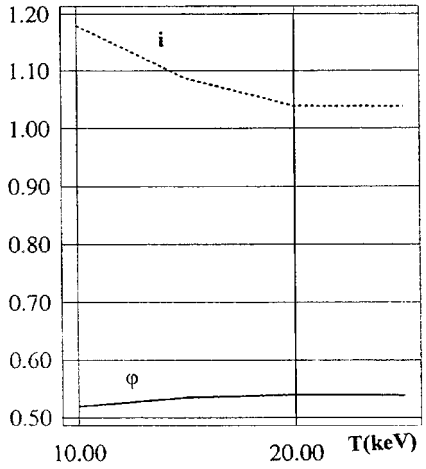

FIG. 8. Burnup fraction φ and tritium index i versus initial bursting temperature, for a target with $x = 0.025$, $\rho = 500$ g/cm^3 and $\rho R = 15$ g/cm^2 (linear scales).

Initial burning temperature and ρR, which are related to each other as depicted in Fig. 4, are the most important parameters to define the catalytic tritium regime. In general, and not only for input energy minimization, it is advisable to start with a bursting temperature as small as possible (i.e. close to the ignition temperature). Otherwise, the burnup fraction increases and the tritium index decreases, as predicted by Eq. (10). This is seen in Fig. 8, for cases with different initial temperatures for a DT$_x$ target with $x = 0.025$, $\rho = 500$ g/cm^3 and $\rho R = 15$ g/cm^2.

The dependence of tritium index on areal density is shown in Figs 9 and 10, for a target with a composition of $x = 0.025$, 500 g/cm^3 density and 10 keV initial bursting temperature. Higher ρR values lead to higher burnup fraction and higher tritium index, because bursting temperature also increases

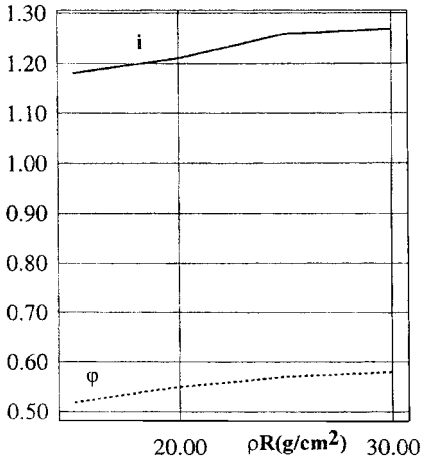

FIG. 9. Tritium index and deuterium burnup fraction versus areal density, for targets with the following common specifications: $x = 0.025$, $T_{ig} = 10$ keV, $\rho = 500$ g/cm^3. The radius of the compressed target was changed between 300 and 600 μm (linear scales).

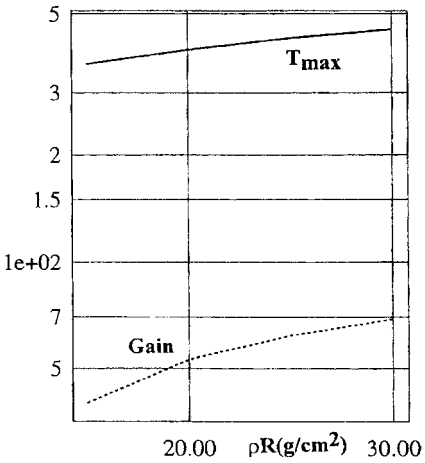

FIG. 10. Maximum burning temperatures and spark gains for the cases described in Fig. 9 (linear scales).

with ρR (in a way very similar to the burnup fraction increase).

Figure 10 also shows the evolution of the spark gain. Note that this is not the actual gain of the target in a propagated ignition target. If the mass of the target is 10 times as large as the spark mass, gain must be multiplied roughly by 10. Although the space–time dependent burnup would have to be solved to calculate the target gain more accurately, the former proportional rule can be taken as a first estimate.

A fundamental problem in relation to areal density is the fuel mass. For $\rho R = 15$ g/cm^2, it is 56 mg at 500 g/cm^3. For $\rho R = 30$ g/cm^2 it rises to 452 mg,

which is too high by any account. The spark mass can be written as

$$M = \frac{4}{3}\,\pi\,\frac{(\rho R)^3}{\rho^2} \tag{68}$$

and for a given ρR it decreases as ρ^{-2}. This is the reason why higher densities could be advisable and even indispensable for actual scenarios. In any case, variations of the tritium index point out that there is a suitable design window for the catalytic regime which is compatible with the specifications of futuristic inertial fusion targets and which will not need any external tritium breeding.

5. SUMMARY AND FUTURE WORK

A property of the DD and DT reaction reactivities has been presented, by means of which catalytic burnup can take place in an inertial fusion target, in a way such that the final tritium content in the pellet debris is the same as the initial content. This makes the breeding of tritium in outer blankets or other machines unnecessary. This property is only relevant at very high burning temperatures and high densities, in clear compatibility with standard inertial fusion target specifications. The general requirements for tritium internal self-breeding were analysed in Section 2, where Eq. (10) summarizes those requirements.

The analyses of Sections 3 and 4 were used to establish the design windows of DT_x plasmas. In order to have appropriate reference points, stoichiometric DT and pure DD targets were also included in the analysis. The main conclusion was that a DT_x plasma with $x = 0.025$ has a much lower ignition temperature than a pure DD plasma and a higher gain. Although both magnitudes are still better for DT (which has the minimum ignition temperature), stoichiometric DT needs a complex process of tritium breeding and reprocessing, involving a large amount of tritium and conveying a serious radiological problem. The tritium inventory could be reduced by 2 orders of magnitude or more, in a tritium breedingless reactor working according to the principles presented in this article.

Future work must focus on improving numerical simulations of these targets, including the implosion phase. Of course, this proposal of using DT_x fuel is not restricted to any type of target scheme, and can be included both in direct drive and indirect drive targets or fast ignitors.

ACKNOWLEDGEMENTS

S.E. is an Iberdrola Chair visiting professor in Madrid. This work was sponsored in part by Spain's Ministry of Culture and Education.

REFERENCES

[1] KESSLER, G., KULCINSKI, G.L., PETERSON, R.R., in Nuclear Fusion by Inertial Confinement, (VELARDE, G., RONEN, Y., MARTÍNEZ-VAL, J.M., Eds), CRC Press, Boca Raton, FL (1993) Ch. 26.
[2] PIET, S.J., et al., in Energy from Inertial Fusion, IAEA, Vienna (1995) Ch. 6.
[3] RASKOB, W., UFOTRI: A Program for Assessing the Offsite Consequences from Accidental Tritium Releases, Rep. KfK 4605, Forschungszentrum Karlsruhe (1991).
[4] RAEDER, J., ITER Safety, ITER Documentation Series No. 36, IAEA, Vienna (1991).
[5] SCAFFIDI-ARGENTINA, F., DALLE DONNE, M., RONCHI, C., FERRERO, C., Fusion Technol. **32** (1997) 179.
[6] ELIEZER, S., HENIS, Z., MARTÍNEZ-VAL, J.M., Nucl. Fusion **37** (1997) 985.
[7] BRUECKNER, K.A., JORNA, S., Rev. Mod. Phys. **46** (1973) 325.
[8] FRALEY, G.S., LINNEBUR, E.J., MASON, R.J., MORSE, R.L., Phys. Fluids **17** (1974) 2.
[9] KIDDER, R.E., Nucl. Fusion **19** (1979) 223.
[10] MEYER-TER-VEHN, J., Nucl. Fusion **22** (1982) 561.
[11] TABAK, M., et al., Phys. Plasmas **1** (1994) 1626.
[12] MARTÍNEZ-VAL, J.M., ELIEZER, S., PIERA, M., Laser Part. Beams **12** (1994) 681.
[13] HORA, H., RAY, P.S., Z. Nat.Forsch. A **33** (1978) 890.
[14] CHU, M.S., Phys. Fluids **15** (1972) 413.
[15] GUSKOV, S.Yu., ROZANOV, V., in Nuclear Fusion by Inertial Confinement (VELARDE, G., RONEN, Y., MARTÍNEZ-VAL, J.M., Eds), CRC Press, Boca Raton, FL (1993) Ch. 12.
[16] GUSKOV, S.Yu., KROKHIN, O.N., ROZANOV, V., Nucl. Fusion **16** (1976) 957.
[17] LINHART, J.G., Nuovo Cimento A **106** (1993) 1949.
[18] LINDL, J.D., Phys. Plasmas **2** (1995) 3933.
[19] ROZANOV, V.B., et al., in Energy from Inertial Fusion, IAEA, Vienna (1995).
[20] NUCKOLLS, J., WOOD, L., ZIMMERMANN, G., THIESSEN, A., Nature **239** (1972) 139.
[21] VELARDE, G., et al., Laser Part. Beams **4** (1986) 349.
[22] MARTÍNEZ-VAL, J.M., RONEN, Y., VELARDE, G., in Nuclear Fusion by Inertial Confinement

(VELARDE, G., RONEN, Y., MARTÍNEZ-VAL, J.M., Eds), CRC Press, Boca Raton, FL (1993) Ch. 1.
[23] LINDL, J.D., McCRORY, R.L, CAMPBELL, E.M., Phys. Today **45** (1992) 32.
[24] TAHIR, N.A., LONG, K.A., Phys. Fluids **30** (1987) 1820.
[25] DUDERSTADT, J.J., MOSES, G., Inertial Confinement Fusion, Wiley, New York (1982).
[26] YABE, T., in Nuclear Fusion by Inertial Confinement (VELARDE, G., RONEN, Y., MARTÍNEZ-VAL, J.M., Eds), CRC Press, Boca Raton, FL (1993) Ch. 11.
[27] McCRORY, R.L., "Laser-driven ICF experiments", ibid., Ch. 22.
[28] YAMANAKA, C., NAKAI, S., Nature **319** (1986) 757.
[29] MIMA, K., TAKABE, H., NAKAI, S., Laser Part. Beams **7** (1989) 249.
[30] BANGERTER, R.O., Fusion Technol. **13** (1988) 348.
[31] FELDBACHER, R., Alternate Energy Physics Program Datalib, Rep. INDC (AUS)-12/G, Tech. Univ. of Graz (1987).
[32] GLASSTONE, S., LOVBERG, R.H., Controlled Thermonuclear Reactions, Krieger Publishers, New York (1975).
[33] ROSE, D.J., CLARK, M.C., Plasmas and Controlled Fusion, MIT Press, Cambridge, MA (1961).
[34] TAHIR, N.A., LONG, K.A., Nucl. Fusion **23** (1983) 887.
[35] McCRORY, R.L, VERDON, C.P., Computer Modelling and Simulation in Inertial Confinement Fusion (CARUSO, A., SINDONI, E., Eds), Editrice Compositori, Bologna (1988).
[36] MARTÍNEZ-VAL, J.M., PIERA, M., Fusion Technol. **32** (1997) 131.
[37] MARTÍNEZ-VAL, J.M., ELIEZER, S., PIERA, M., VELARDE, G., Phys. Lett. A **216** (1996) 142.
[38] MARTÍNEZ-VAL, J.M., Fusion Technol. **17** (1990) 476.
[39] BOOK, D.L., NRL Plasma Formulary, Naval Research Lab., Washington, DC (1987).
[40] ZINAMON, Z., in Nuclear Fusion by Inertial Confinement (VELARDE, G., RONEN, Y., MARTÍNEZ-VAL, J., Eds), CRC Press, Boca Raton, FL (1993) Ch. 5.
[41] HONRUBIA, J.J., ibid., Ch. 9.
[42] MILEY, G.H., in Laser Interactions and Related Plasma Phenomena, Vol. 5, Plenum Press, New York and London (1981) 313.
[43] RAGHEB, M., MILEY, G.H., Fusion Technol. **8** (1985) 206.
[44] TAZIMA, T., et al., in Plasma Physics and Controlled Nuclear Fusion Research 1986 (Proc. 11th Int. Conf. Kyoto, 1986), Vol. 3, IAEA, Vienna (1986) 343.
[45] HARMS, A.A., HEINDLER, M., Nuclear Energy Synergetics, Plenum Press, New York and London (1982).
[46] DAWSON, J.M., Fusion, Vol. 1, Part B, Academic Press, New York (1981) Ch. 16.

(Manuscript received 11 February 1998
Final manuscript accepted 13 August 1998)

E-mail address of J.M. Martínez-Val:
mval@etsii.upm.es

Subject classification: A0, L0